

## Observation of a midinfrared band in SrTiO<sub>3-y</sub>

P. Calvani, M. Capizzi, F. Donato, S. Lupi, P. Maselli, and D. Peschiaroli

*Dipartimento di Fisica, Università di Roma "La Sapienza," Piazzale Aldo Moro 2, I-00185 Roma, Italy*

(Received 24 July 1992)

Transmission measurements have been performed in reduced SrTiO<sub>3</sub> between 300 and 17 K for different concentrations of oxygen vacancies. A midinfrared absorption band has been observed, whose behavior with doping and temperature is accounted for by an intraband scattering process, phonon or disorder assisted. Connections with the family of high- $T_c$  superconducting oxides are demonstrated.

### I. INTRODUCTION

SrTiO<sub>3</sub> is a prototype of the  $ABO_3$  perovskite family from which all standard high-critical-temperature ( $T_c$ ) superconductors are derived. It can be easily grown with a low concentration of point defects, and then treated in a reducing atmosphere to produce a controlled amount of oxygen vacancies in a wide range of concentrations. SrTiO<sub>3</sub> is a wide-gap insulator, well described in a tight-binding approach,<sup>1-3</sup> with a cubic structure at room temperature, tetragonal below  $\sim 110$  K.<sup>4</sup> When doped with oxygen vacancies or Nb, SrTiO<sub>3</sub> shows an  $n$ -type conductivity,<sup>5</sup> which turns into  $n$ -type superconductivity at high doping levels and  $T < 1$  K.<sup>6,7</sup> To our knowledge, no antiferromagnetism has ever been detected in SrTiO<sub>3</sub>, whose superconducting behavior has been accounted for in terms of conventional BCS theory.<sup>6-9</sup> Nevertheless, it has been recently pointed out that the Migdal approximation does not hold in materials where the Fermi energy is comparable with the energy of the phonon exchanged in a BCS pair.<sup>9</sup> This raises serious doubts about the possibility of applying a conventional BCS approach to SrTiO<sub>3</sub>. Moreover, this material singles out within the family of normal superconductors for several experimental aspects: First, its  $T_c$  goes through a maximum as a function of the carrier density  $n$ ,<sup>6-8</sup> much like that of high- $T_c$  superconductors (HTCS's), e.g.,  $n$ -type Nd<sub>2-x</sub>Ce<sub>x</sub>CuO<sub>4</sub> (Ref. 10) and  $p$ -type La<sub>2-x</sub>Sr<sub>x</sub>CuO<sub>4</sub>,<sup>11</sup> second, the maximum  $T_c$  of SrTiO<sub>3-y</sub> is comparable to that of Zn, a BCS superconductor whose  $n$  exceeds that of strontium titanate by more than 3 orders of magnitude.

The above arguments are further supported by inspection of Figs. 1 and 2. In Fig. 1 we report the 4-K electrical conductivity  $\sigma_{dc}$  and the corresponding carrier density  $n$ , as measured by different authors in a number of SrTiO<sub>3-y</sub> samples.<sup>7,12-14</sup> As one can see,  $\sigma_{dc}$  increases by 5 orders of magnitude as  $n$  changes from  $\sim 10^{17}$  to  $\sim 2 \times 10^{18}$  cm<sup>-3</sup>. Even if additional data in the insulating phase would be helpful, such an abrupt change clearly indicates the occurrence in SrTiO<sub>3-y</sub> of an insulator-to-metal transition determined by oxygen defects, analogous to those induced by doping in charge-transfer

HTCS's such as Nd<sub>2-x</sub>Ce<sub>x</sub>CuO<sub>4</sub> and La<sub>2-x</sub>Sr<sub>x</sub>CuO<sub>4</sub>. In SrTiO<sub>3-y</sub> the transition is not as sharp as could be expected, probably due to strong density fluctuations in the distribution of defects.

In Fig. 2, values of  $T_c$  and of  $n^{2/3}/(m^*/m_0)$  for SrTiO<sub>3-y</sub>, where  $m^*=5m_0$  is the effective mass of the carriers and  $m_0$  is the electron mass,<sup>7</sup> have been added to a plot recently proposed<sup>15</sup> by Uemura *et al.* SrTiO<sub>3</sub> data<sup>6,7</sup> (solid circles) look consistent with those of HTCS's, Chevrel phases (CP's) and heavy fermion (HF) families, while no clear correlation with normal, elemental superconductors (NS's) is found.

From the point of view of optical properties, a further similarity is given by the observation in SrTiO<sub>3-y</sub> of an absorption band in the midinfrared.<sup>13,16-18</sup> A contribution to the optical conductivity, which adds to the Drude one in the metallic phase and can be modeled by a broad oscillator in the midinfrared (MIR), the so-called MIR band, has in fact been observed in all HTCS's. Both in  $n$ -type Nd<sub>2-x</sub>Ce<sub>x</sub>CuO<sub>4</sub> (Refs. 10 and 19) and  $p$ -type La<sub>2-x</sub>Sr<sub>x</sub>CuO<sub>4</sub>,<sup>11</sup> the midinfrared band arises at a dop-

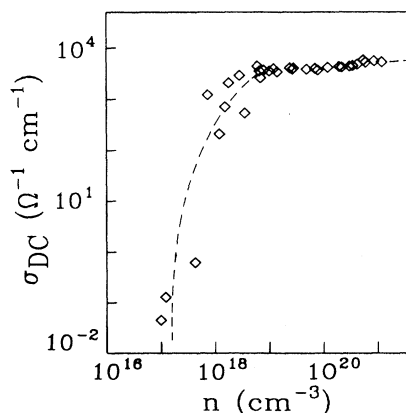


FIG. 1. Conductivity of SrTiO<sub>3</sub> at liquid helium temperature as a function of the room-temperature free-carrier concentration. Data are taken from Refs. 7, 12, 13, and 14. The line is just a guide to the eye.

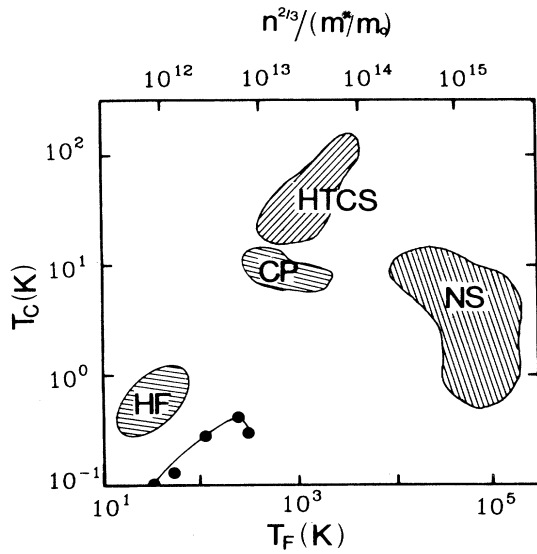


FIG. 2. Log-log plot of  $T_c$  vs  $n^{(2/3)}/(m^*/m_0)$  for  $\text{SrTiO}_3$ , as from data of Ref. 7 (solid circles). The solid line is a guide to the eye. Data for HTCS's, Chevrel phases (CP's), normal superconductors (NS's), and heavy fermions (HF's) are also schematically shown, as taken from Ref. 15.

ing level which is low compared to those characteristic of the metallic phase. The MIR band persists in the metallic phase on top of the conventional Drude absorption, its intensity not depending appreciably on temperature. The origin of this band has been attributed to Holstein processes,<sup>20</sup> Holstein-like processes involving magnons,<sup>21</sup> the effect of doping on charge-transfer transitions,<sup>22</sup> a marginal Fermi liquid,<sup>23</sup> and peculiar correlation effects in doped charge-transfer insulators.<sup>24</sup> Recently, it has also been suggested that oxygen vacancies may explain the insurgence of the MIR band.<sup>25,26</sup>

In this paper a detailed investigation of the midinfrared spectrum of  $\text{SrTiO}_3$  has been carried out. It is aimed at a better understanding of the infrared optical properties of this material and also at getting, within the above scenario, more detailed information on the electronic properties of high- $T_c$  superconductors.

## II. EXPERIMENT

The  $\text{SrTiO}_3$  samples, all cut from a single crystal grown by National Lead Co., were carefully polished. Two out of them were kept as grown; the others were annealed under vacuum or in a reducing  $\text{N}_2$  atmosphere after having been thinned down. An oxygen-vacancy desorption has been observed in samples which have been processed in the reverse order. Four-wire conductivity measurements have been performed by evaporating gold contacts on all samples. Thickness, temperature, and length of the annealing process, as well as room-temperature dc conductivity, are reported in Table I for all samples prepared by us. A further sample was examined (*D*) which had been reduced long time ago in a  $\text{H}_2$  atmosphere for thermomodulated optical absorption measurements.<sup>27</sup> This sample, 288  $\mu\text{m}$  thick, has  $\sigma_{\text{dc}} = 0.07 \Omega^{-1}\text{cm}^{-1}$ . Values of the free-carrier density  $n$  at room temperature, as obtained by comparison with a calibration derived from data of Ref. 17 [ $n(10^{18} \text{cm}^{-3}) = A\sigma_{\text{dc}}$ , with  $A \simeq 1 \Omega \text{cm}^{-2}$ ], are also listed in Table I.

Optical reflectivity and transmittance measurements were performed by a rapid scanning interferometer. Observation of room-temperature reflectance spectra, not shown here, was attempted on a few samples. The mid-infrared absorption turned out to be very weak, and it could not be conveniently studied; strong phonons, only slightly shielded in the most reduced samples, were instead observed in the far infrared. We then performed transmission measurements in the energy range from 800 to 26000  $\text{cm}^{-1}$ , by mounting the samples on the coldest flange of a two-stage closed-cycle cryostat equipped with KRS-5 and quartz windows. The temperature was controlled and measured within 1 K by means of heaters and of platinum thermometers.

## III. RESULTS AND DISCUSSION

Transmission spectra obtained for some of the samples described in Table I are reported by solid circles on a log-linear scale in Fig. 3. The transmission is vanishingly small, on the low-energy side, due to the presence of very strong phonons<sup>28,29</sup> and, on the high-energy side, due to the proximity of the optical gap.<sup>1-3,30</sup> The energy range can be tentatively divided into two regions 800-

TABLE I. Thickness  $d$  and annealing conditions (temperature  $T_a$ , length  $\Delta t_a$ , and atmosphere At) for the samples studied in the present work. Values of room-temperature dc conductivity, as determined by four wire measurements, and of the carrier concentration  $n$ , as extracted from  $\sigma_{\text{dc}}$  by using the calibration of Ref. 14, are also given.

Sample	$d$ ( $\mu\text{m}$ )	$T_a$ ( $^\circ\text{C}$ )	$\Delta t_a$ (h)	At	$\sigma_{\text{dc}}$ [ $\Omega \text{cm}^{-1}$ ]	$n$ ( $\text{cm}^{-3}$ )
<i>N</i>	2300				$1.1 \times 10^{-8}$	$10^{10}$
<i>M</i>	278				$5 \times 10^{-8}$	$5 \times 10^{10}$
<i>M''</i>	278	750	0.5	$\text{N}_2$	$2 \times 10^{-4}$	$2 \times 10^{14}$
<i>B</i>	520	900	0.25	$\text{N}_2$	0.25	$2.5 \times 10^{17}$
<i>E'</i>	140	900	2.25	$\text{N}_2$	0.5	$5 \times 10^{17}$
<i>P</i>	30	1150	12.0	Vacuum	2.2	$2 \times 10^{18}$

TABLE II. Values of the oscillator parameters  $\Omega$  and  $\Gamma$ , expressed in  $\text{cm}^{-1}$ , and  $S^2$ , in  $\text{cm}^{-2}$ , for the lightly doped sample  $M''$ . A value of 2.5 has been used for  $\epsilon_\infty$  to fit Eq. (1) to the data.

	1320	1800	2150	4400	7000	14 500	20 000	23 600	26 000
$\Omega$	1320	1800	2150	4400	7000	14 500	20 000	23 600	26 000
$\Gamma$	50	140	170	1800	6500	12 500	5800	3000	130
$S^2$	800	480	20	180	4530	14 000	9000	5200	45 300

8000  $\text{cm}^{-1}$  and 8000–26 000  $\text{cm}^{-1}$ . In the latter, transitions from energy levels of residual impurities<sup>13,14,31</sup> give rise to the structures observed at 7000, 14 500, 20 000, and 23 600  $\text{cm}^{-1}$ . In the former, several narrow bands are observed in the untreated sample, not shown in the figure, and in reduced samples, which exhibit no appreciable dependence on doping. The nature of these bands, the strongest one being at 1320  $\text{cm}^{-1}$ , is still controversial in spite of a large number of theoretical and experimental studies.<sup>17,32–36</sup> The main object of the present investigation is the study of a broadband which appears in the midinfrared as soon as doping becomes sizable ( $\sigma_{\text{dc}} \geq 10^{-3} \Omega^{-1} \text{cm}^{-1}$ ).

In order to make a quantitative analysis of these bands, transmission spectra were fitted by a Lorentz dielectric function<sup>18,19,37</sup>

$$\begin{aligned} \tilde{\epsilon}(\omega) = \epsilon_\infty + & \sum_j \frac{S_j^2}{(\omega_j^2 - \omega^2) - i\omega\Gamma_j} \\ & + \frac{S_{\text{MIR}}^2}{(\omega_{\text{MIR}}^2 - \omega^2) - i\omega\Gamma_{\text{MIR}}} \\ & + \sum_i \frac{S_G^2}{(\omega_G^2 - \omega^2) - i\omega\Gamma_G}. \end{aligned} \quad (1)$$

The contributions to  $\tilde{\epsilon}(\omega)$  are given by phonons and defects of frequencies  $\omega_j$ , linewidths  $\Gamma_j$ , and strengths  $S_j$ , one (or more) midinfrared (MIR) oscillator(s) at  $\omega_{\text{MIR}}$ , the optical gap at  $\omega_G$ ,<sup>38</sup> and finally  $\epsilon_\infty$ , which includes all higher-energy transitions. Even for the sample with the highest conductivity in Fig. 3, the concentration of oxygen vacancies is low enough to give an appreciable

free-carrier absorption only at frequencies below the investigated range, and therefore the Drude term has not been considered in Eq. (1).

The solid lines in Fig. 3 are the results of best fits to data of reduced samples. The values obtained for the oscillator parameters are reported in Table II in the case of the lightly doped  $M''$  sample. The agreement with previous results<sup>13,14,31</sup> is good. One can notice that oscillators  $\alpha$  at 2150  $\text{cm}^{-1}$  and  $\beta$  at 4400  $\text{cm}^{-1}$  are very weak in this sample. Further  $\alpha$  and  $\beta$  values are reported in Table III for samples with higher  $\sigma_{\text{dc}}$  and  $n$ . Both oscillators become increasingly intense as doping is increased, while their peak frequencies are always found at  $\sim 2300$  and  $\sim 4000$   $\text{cm}^{-1}$ , respectively. Since they show a similar dependence on  $n$ , from now on they will be considered to describe a single, structured MIR band whose strength  $S_{\text{MIR}}^2$  is given vs  $\sigma_{\text{dc}}$  in Fig. 4. The linear behavior observed for  $S_{\text{MIR}}^2$  can be explained either in terms of transitions starting from localized levels, possibly related to the oxygen vacancy, or in terms of intraband scattering between delocalized levels. In the latter case, the defect states act as a reservoir of carriers. In order to discriminate between these two mechanisms, measurements of midinfrared transmission as a function of temperature have been performed: As the temperature increases, the absorption due to transitions from oxygen vacancy levels would indeed decrease, while that resulting from intraband scattering would increase. A direct inspection of Fig. 5 indicates that the latter mechanism is more likely. The transmittance of sample  $E'$  shows indeed a strong decrease with  $T$ , observed also for samples  $P$  and  $D$ , not shown here.<sup>33–36</sup>

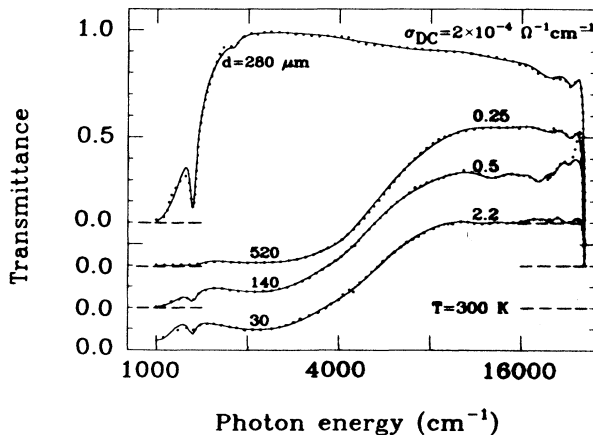


FIG. 3. Room-temperature transmittance of SrTiO<sub>3</sub> vs photon energy for samples with different conductivity  $\sigma_{\text{dc}}$  and thickness  $d$

TABLE III. Energies  $\Omega$  and widths  $\Gamma$ , in  $\text{cm}^{-1}$ , and strengths  $S^2$ , in  $\text{cm}^{-2}$ , of the midinfrared oscillators  $\alpha$  and  $\beta$  for samples with various carrier concentrations  $n$ .

Sample	$n$ ( $10^{18} \text{cm}^{-3}$ )			
		$\alpha$	$\beta$	
$D$	0.07	$\Omega$	2305	4085
		$\Gamma$	2450	2000
		$S^2$	50 050	3900
$B$	0.25	$\Omega$	2300	3950
		$\Gamma$	2380	1980
		$S^2$	49500	3670
$E'$	0.5	$\Omega$	2330	4050
		$\Gamma$	2400	2500
		$S^2$	116 000	17000
$P$	2.2	$\Omega$	2300	3950
		$\Gamma$	2700	2800
		$S^2$	565 000	68000

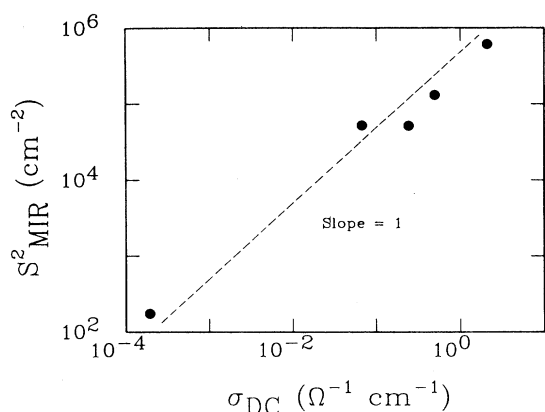


FIG. 4. Logarithmic plot of the intensity  $S_{\text{MIR}}^2$  of the mid-infrared band vs the sample dc conductivity. Both quantities are measured at room temperature.

A quantitative study of the behavior of the MIR band with temperature has been performed by fitting the transmission data at different  $T$  to Eq. (1) (a typical fit has been already shown in Fig. 3 for the 300-K data). The total intensity  $S_{\text{MIR}}^2$  of the MIR band is plotted vs  $1/T$  for samples  $D$  (circles),  $E'$  (squares), and  $P$  (crosses) in Fig. 6. The behavior of  $S_{\text{MIR}}^2$  is strikingly similar to that of  $1/R_H$  vs  $1/T$ , where  $R_H$  is the Hall coefficient measured in reduced samples of comparable conductivities by Lee, Destry, and Brebner.<sup>13</sup> A change of slope can also be observed at temperatures close to that of the cubic-to-tetragonal transition ( $\sim 110$  K). In Fig. 6, a good fit of  $S_{\text{MIR}}^2$  over the whole temperature range can be obtained by

$$S_{\text{MIR}}^2 = A + Be^{-\Delta/T}. \quad (2)$$

Values of  $A$ ,  $B$ , and  $\Delta$  in Eq. (2) are given in Table IV. As one can see,  $A$  is roughly linearly dependent on  $n$  and is independent of  $T$ ,  $B$  is independent of  $n$ , and  $\Delta$  decreases with  $n$ .

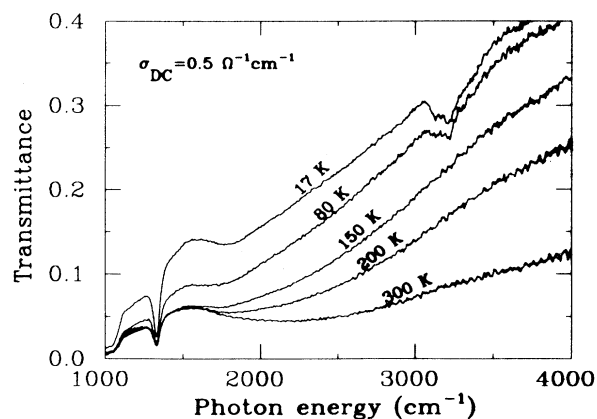


FIG. 5. Transmittance of sample  $E'$  vs photon energy at different temperatures.

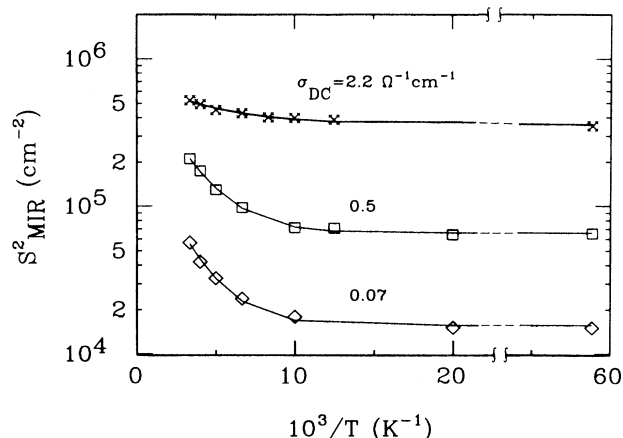


FIG. 6. Intensity  $S_{\text{MIR}}^2$  of the midinfrared band vs inverse temperature for samples with different dc conductivities. Solid lines are the results of best fits to Eq. (2). The parameters of the fits are given in Table IV.

The above results cast serious doubts on the polaronic model, earlier invoked to account for the midinfrared absorption in  $\text{SrTiO}_3$ .<sup>17,39–41</sup> Indeed, any increase in temperature or doping would lead to a decrease in the band strength, via an increased screening of free carriers,<sup>17,41</sup> contrary to what is observed here. The temperature-independent contribution  $A$  to the MIR band as well as its linear dependence on the carrier concentration may be explained if the details of the conduction band dispersion are taken into account. In  $\text{SrTiO}_3$ , this band has two minima, at the  $\Gamma$  and at the  $X$  point. Although the relative order of the energy of these two valleys has been the object of a long, still unresolved theoretical and experimental controversy,<sup>30</sup> a general consensus exists on the width of the conduction band in the  $[100]$  direction,<sup>2,3</sup> which should be  $1600 \pm 800 \text{ cm}^{-1}$ . An electron scattering process between these two valleys, phonon and/or disorder assisted, would then have a characteristic energy in substantial agreement with that of the present MIR band. In the case of no-phonon processes (disorder assisted transitions), the relaxation of the  $\mathbf{k}$ -selection rule would be due to the breaking of the translational symmetry caused by the high doping. Moreover, the high electron effective mass theoretically predicted along the  $[100]$  direction<sup>1–3</sup> would give rise to a high joint density of states, thus making the absorption process quite strong.

As far as the temperature-dependent contribution is concerned, one would be tempted to ascribe it to a remnant of phonon-assisted processes: A strong coupling of free carriers to phonons has been observed in inelastic tunneling,<sup>42</sup> infrared reflectivity,<sup>39</sup> optical absorption,<sup>30</sup> and conductivity measurements.<sup>43</sup> This strong coupling has been also predicted by theoretical estimates.<sup>41</sup> However, this attribution is unsatisfactory, because the activation energies  $\Delta$  measured here depend on  $n$  and are much lower than those of the two highest longitudinal optical modes which more strongly couple with electrons ( $470$  and  $810 \text{ cm}^{-1}$ , at the  $\Gamma$  point). On the other hand, if the thermally activated component of the MIR band were due to a change in the free-carrier population of the

TABLE IV. Parameters of Eq. (2), as obtained from the fit to data in Fig. 6.

Sample	$n$ ( $10^{18}\text{cm}^{-3}$ )	$A$ ( $10^4\text{cm}^{-2}$ )	$B$ ( $10^4\text{cm}^{-2}$ )	$\Delta$ ( $\text{cm}^{-1}$ )
<i>D</i>	0.07	1.6	22	360
<i>E'</i>	0.5	6.6	69	320
<i>P</i>	2.2	36	35	160

initial state, i.e., to transitions from an impurity level to the conduction band, the samples would be insulating and the impurity binding energy should be equal to the activation energy. The coexistence of two fluids, the former consisting of free carriers, the latter of bound charges, is made possible by strong density fluctuations like those suggested by the large width of the metal-to-insulator transition in Fig. 1. The free-carrier density measured at room temperature in our samples place them just at the top of the transition region from a purely insulating behavior ( $n \leq 10^{17}\text{cm}^{-3}$ ) to a purely metallic one ( $n \geq 2 \times 10^{18}\text{cm}^{-3}$ ). The metallic fraction of the sample would then account for the temperature-independent term, linear with  $n$ , the insulating fraction for the temperature dependent one. The thermal activation energy, equal to the impurity binding energy in the limit of highly diluted impurities, approaches zero for impurity concentrations attaining the insulator-to-metal transition, in agreement with the concentration dependence reported for  $\Delta$  in Table IV. On the insulating side, for an infinitely diluted sample, the absorption measured at  $1320\text{cm}^{-1}$  was found to be thermally activated with an activation energy<sup>44</sup> equal to  $600 \pm 75\text{cm}^{-1}$ . Our data show that the narrow oscillator at  $1320\text{cm}^{-1}$  is  $T$  independent. Assuming that the temperature dependence observed in Ref. 44 comes from the broad MIR band at higher energy, one finds that  $\Delta = 600\text{cm}^{-1}$  is consistent with the results of Table IV. The latter value should then give a measure of the binding energy of the oxygen vacancy, to be compared with a tight-binding evaluation of  $970\text{cm}^{-1}$  for this quantity in the case of a neutral vacancy.<sup>45</sup>

#### IV. CONCLUSION

This work has been aimed at identifying similarities and differences between the midinfrared absorption observed in  $\text{SrTiO}_{3-y}$  and the midinfrared band of high- $T_c$  superconducting cuprates. Such a comparison is physically meaningful for the following reasons: (i) Doped  $\text{SrTiO}_3$ , like some HTCS's, undergoes an insulator-to-metal transition, which we believe to occur at  $\sigma_{dc} \sim 1\Omega^{-1}\text{cm}^{-1}$  or  $n \sim 10^{18}\text{cm}^{-3}$ ; (ii) it exhibits a superconducting phase in a well-defined region of the  $(n, T)$  plane; (iii) even if in  $\text{SrTiO}_{3-y}$  the absolute value of  $T_c$  is  $< 1\text{K}$ , the ratio  $T_c/n$  is of the same order as in HTCS's because of the relatively small value of the carrier concentration ( $n \sim 10^{19}\text{cm}^{-3}$ ). On the other hand,  $\text{SrTiO}_3$  is different from the parent compounds of HTCS's in that the latter ones are charge-transfer insulators and have antiferromagnetic Cu-O planes, while the former is a conventional insulator. As already recalled, the origin of the midinfrared

band in HTCS's (which in their metallic phases yields the well-known additional contribution over the Drude absorption) is still an open question. The existence of a MIR band in  $\text{SrTiO}_{3-y}$  offers the opportunity of studying this interesting feature in a superconducting oxide having a very low density of carriers. This allows performing accurate transmission measurements in the midinfrared, in the virtual absence of Drude absorption.

Our results can be summarized as follows. A midinfrared absorption is confirmed to be present in  $\text{SrTiO}_3$  after the reduction process. It can be modeled by two Lorentzian oscillators centered at  $2300$  and  $4000\text{cm}^{-1}$ , the former being much more intense than the latter. In analogy with  $\text{Nd}_{2-x}\text{Ce}_x\text{CuO}_4$  (Ref. 19) and  $\text{La}_{2-x}\text{Sr}_x\text{CuO}_4$ ,<sup>11</sup> where the MIR band is centered at  $\sim 4000\text{cm}^{-1}$ , that of  $\text{SrTiO}_3$  appears at very low doping and is observed well below the insulator-to-metal transition. At room temperature, the intensity of the MIR band is proportional to the carrier density  $n$ . It is also markedly dependent on temperature at low doping, but it tends to become independent of  $T$  as the sample approaches the metallic phase (see Fig. 6). As far as we know, no detailed measurements of  $S_{\text{MIR}}^2$  vs  $T$  are available for HTCS's. Nevertheless, in the metallic phases of  $\text{YBa}_2\text{Cu}_3\text{O}_{7-y}$ ,<sup>46</sup> the MIR band is also found to be independent of  $T$ . From all the above results, we get a strong indication that the MIR band of  $\text{SrTiO}_{3-y}$  has the same origin as the one observed in high- $T_c$  superconducting cuprates.

In the literature, the MIR band of  $\text{SrTiO}_{3-y}$  has been explained in the framework of a polaronic model. This model is not supported by our data, as it can hardly explain the linear increase of  $S_{\text{MIR}}^2$  with the free-carrier concentration  $n$ . In alternative, we suggest that in  $\text{SrTiO}_{3-y}$  the MIR band is due to intraband scattering processes, related to the existence of a second minimum in the conduction band. In HTCS's, where the parent compounds are charge-transfer insulators, the MIR band intensity should increase linearly with doping only at very low impurity concentrations. At higher concentrations, the indirect action of doping which consists in a massive transfer of states from the charge-transfer band<sup>19</sup> to lower energies becomes more important. The latter effect, which greatly increases the number of carriers available at the insulator-to-metal transition, may be the main reason for the dramatic difference in the critical temperature between superconducting cuprates and  $\text{SrTiO}_3$ .

#### ACKNOWLEDGMENTS

This work was supported by Progetto SATT of Consorzio INFN, and by Progetto Finalizzato Superconduttività of Consiglio Nazionale delle Ricerche.

- <sup>1</sup>A.H. Kahn and A.J. Leyendecker, *Phys. Rev.* **135**, A1321 (1964).
- <sup>2</sup>L.F. Mattheiss, *Phys. Rev. B* **6**, 4718 (1972); **6**, 4740 (1972).
- <sup>3</sup>T.F. Soules, E.J. Kelly, D.M. Vaught, and J.W. Richardson, *Phys. Rev. B* **6**, 1519 (1972).
- <sup>4</sup>F.W. Lytle, *J. Appl. Phys.* **35**, 2212 (1964); T. Sakudo and H. Unoki, *Phys. Rev. Lett.* **26**, 851 (1971).
- <sup>5</sup>J.F. Schooley, W.R. Hosler, and M.L. Cohen, *Phys. Rev. Lett.* **12**, 474 (1964).
- <sup>6</sup>J.F. Schooley, W.R. Hosler, E. Ambler, J.H. Becker, M.L. Cohen, and C.S. Koonce, *Phys. Rev. Lett.* **14**, 305 (1965).
- <sup>7</sup>C.S. Koonce, M.L. Cohen, J.S. Schooley, W.R. Hosler, and E.R. Pfeiffer, *Phys. Rev.* **163**, 380 (1967).
- <sup>8</sup>G. Binnig, A. Baratoff, H.E. Hoenig, and J.G. Bednorz, *Phys. Rev. Lett.* **45**, 1352 (1980).
- <sup>9</sup>L. Pietronero, *Europhys. Lett.* **17**, 365 (1992).
- <sup>10</sup>S. Uchida, *Mod. Phys. Lett. B* **4**, 513 (1990); H. Takagi, S. Uchida, and Y. Tokura, *Phys. Rev. Lett.* **62**, 1197 (1989).
- <sup>11</sup>S. Uchida, T. Ido, H. Takagi, T. Arima, Y. Tokura, and S. Tajima, *Phys. Rev. B* **43**, 7942 (1991).
- <sup>12</sup>O.N. Tufte and P.W. Chapman, *Phys. Rev.* **155**, 796 (1967).
- <sup>13</sup>C. Lee, J. Destry, and J.L. Brebner, *Phys. Rev. B* **11**, 2299 (1975).
- <sup>14</sup>G. Perluzzo and J. Destry, *Can. J. Phys.* **56**, 453 (1978).
- <sup>15</sup>Y. J. Uemura, L. P. Le, G. M. Luke, B. J. Sternlieb, W. D. Wu, J. H. Brewer, T. M. Riseman, C. L. Seaman, M. P. Maple, M. Ishikawa, D. G. Hinks, J. D. Jorgensen, G. Saito, and H. Yamochi, *Phys. Rev. Lett.* **66**, 2665 (1991).
- <sup>16</sup>W. S. Baer, *Phys. Rev.* **144**, 734 (1966).
- <sup>17</sup>E.V. Bursian, Ya.G. Girshberg, and A.V. Ruzhnikov, *Fiz. Tverd. Tela (Leningrad)* **18**, 578 (1976) [*Sov. Phys. Solid State* **18**, 335 (1976)].
- <sup>18</sup>T. Timusk and D.B. Tanner, in *Physical Properties of High Temperature Superconductors*, edited by D.M. Ginsberg (World Scientific, Singapore, 1989), pp. 339-407, and references therein.
- <sup>19</sup>S. Lupi, P. Calvani, M. Capizzi, P. Maselli, W. Sadowski, and E. Walker, *Phys. Rev. B* **45**, 12470 (1992); P. Calvani, M. Capizzi, S. Lupi, P. Maselli, D. Peschiaroli, and H. Katayama-Yoshida, *Solid State Commun.* **74**, 1333 (1990).
- <sup>20</sup>S. L. Cooper, G. A. Thomas, J. Orenstein, D. H. Rapkine, M. Capizzi, T. Timusk, A. J. Millis, L. F. Schneemeyer, and J. V. Waszczak, *Phys. Rev. B* **40**, 11358 (1989).
- <sup>21</sup>C. X. Chen and H. B. Schüttler, *Phys. Rev. B* **43**, 3771 (1991).
- <sup>22</sup>I. Terasaki, T. Nakahashi, S. Takebayashi, A. Maeda, and K. Uchinokura, *Physica C* **165**, 152 (1990).
- <sup>23</sup>C. M. Varma, P. B. Littlewood, S. Schmitt-Rink, E. Abrahams, and A. E. Rukenstein, *Phys. Rev. Lett.* **63**, 1996 (1989).
- <sup>24</sup>H. Eskes, M.B. Meinders, and A. Sawatzky, *Phys. Rev. Lett.* **67**, 1035 (1991); E. Dagotto, A. Moreo, F. Ortolani, D. Poiblanc, and J. Riera, *Phys. Rev. B* **45**, 10741 (1992).
- <sup>25</sup>G. A. Thomas, S. L. Cooper, J. Orenstein, D. H. Rapkine, A. J. Millis, J. V. Waszczak, and L. F. Schneemeyer, *Supercond. Sci. Technol.* **4**, 5235 (1991).
- <sup>26</sup>G. A. Thomas, D. H. Rapkine, S. L. Cooper, S.-W. Cheong, A. S. Cooper, L. F. Schneemeyer, and J. V. Waszczak, *Phys. Rev. B* **45**, 474 (1992).
- <sup>27</sup>M. Capizzi and A. Frova, *Phys. Rev. Lett.* **29**, 1741 (1972).
- <sup>28</sup>A.S. Barker, Jr., *Phys. Rev.* **145**, 391 (1966).
- <sup>29</sup>G.L. Servoin, Y. Luspain, and F. Gervais, *Phys. Rev. B* **22**, 5501 (1980).
- <sup>30</sup>M. Capizzi and A. Frova, *Phys. Rev. Lett.* **25**, 1298 (1970).
- <sup>31</sup>N.N. Lebedeva, A.G. Arushanov, N.S. Pokasova, and M.S. Gadgiev, *Ferroelectrics* **83**, 141 (1988).
- <sup>32</sup>M.I. Cohen, R.C. Casella, R.F. Blunt, and R.A. Forman, *Phys. Rev.* **186**, 834 (1969).
- <sup>33</sup>The weak band at  $\sim 3200 \text{ cm}^{-1}$ , which can be deconvoluted in a number of narrow lines, has been already observed in nominally undoped samples and attributed to H impurities (see Refs. 34–36). Although a detailed investigation of these lines is beyond the scope of the present work, it has to be mentioned that in the present study they appear only for temperatures lower than  $\sim 120 \text{ K}$ , in disagreement with previous reports.
- <sup>34</sup>A.F.W. Klukhuhn, J. Bruining, B. Klootwijk, and J. Van der Elsken, *Phys. Rev. Lett.* **25**, 380 (1970).
- <sup>35</sup>J.L. Brebner, S. Jandl, and Y. Lépine, *Phys. Rev. B* **23**, 3816 (1981).
- <sup>36</sup>D. Houde, Y. Lepine, C. Pepine, S. Jandl, and J.L. Brebner, *Phys. Rev. B* **35**, 4948 (1987).
- <sup>37</sup>A better fit to data has been obtained by introducing an exponential tail for energies differing by more than  $20\Gamma$  from the peak frequency of the Lorentzian oscillator.
- <sup>38</sup>At room temperature, the absorption coefficient of  $\text{SrTiO}_3$  shows an Urbach's tail (Ref. 30). The modelization of the optical edge with a Lorentz oscillator does not affect the results presented in this work.
- <sup>39</sup>A.S. Barker, Jr., in *Optical Properties and Electronic Structure of Metals and Alloys*, edited by F. Abeles (North-Holland, Amsterdam, 1976), p. 453.
- <sup>40</sup>H.G. Reik, *Z. Phys.* **203**, 346 (1967).
- <sup>41</sup>D.M. Eagles and P. Lalouis, *J. Phys. C* **17**, 655 (1984).
- <sup>42</sup>Z. Sroubek, *Solid State Commun.* **7**, 1561 (1969).
- <sup>43</sup>A. Baratoff and G. Binnig, *Physica* **108B**, 1335 (1981).
- <sup>44</sup>P. Rochon, J.L. Brebner, and D. Matz, *Solid State Commun.* **29**, 63 (1979).
- <sup>45</sup>M.O. Selme and P. Pecheur, *J. Phys. C* **16**, 2559 (1983).
- <sup>46</sup>J. Orenstein, G. A. Thomas, S. L. Cooper, D. H. Rapkine, T. Timusk, L. F. Schneemeyer, and J. V. Waszczak, *Phys. Rev. B* **42**, 6342 (1990).